

Dopant Concentration Effect on NiO-doped Sodium Metaphosphate Glasses: A Combined X-Ray Absorption Fine Structure (XAFS) and UV/VIS/NIR Spectroscopic Investigation

Boris Brendebach^a, Robert Glaum^b, Michael Funke^b, Felix Reinauer^b, Josef Hormes^c, and Hartwig Modrow^a

^a Physikalisches Institut, Universität Bonn, Nußallee 12, D-53115 Bonn, Germany

^b Institut für Anorganische Chemie, Universität Bonn, Gerhard-Domagk-Str. 1, D-53121 Bonn, Germany

^c Center for Advanced Microstructures and Devices, 6980 Jefferson Hwy., Baton Rouge, LA 70806, USA

Reprint requests to Dr. H. M.; Fax: +49 228 737869; E-mail: modrow@physik.uni-bonn.de

Z. Naturforsch. **60a**, 449–458 (2005); received March 2, 2005

NiO-doped sodium metaphosphate glasses $(\text{NaPO}_3)_{1-x}(\text{NiO})_x$ ($0.008 \leq x \leq 0.30$) show a color shift from yellow to orange-brown with increasing NiO concentration. XANES and EXAFS spectra of these glasses suggest the presence of $[\text{Ni}^{\text{II}}\text{O}_6]$ groups as chromophores. EXAFS (Ni K-edge) analysis of the NiO-doped phosphate glasses including an evaluation of higher coordination shells leads to $d_{\text{av}}(\text{Ni-O}) = 2.06(2)$ Å. Evidence is provided for an increased connectivity of $[\text{Ni}^{\text{II}}\text{O}_6]$ chromophores at higher NiO concentration in the glasses. A decrease in the intensity of the main absorption edge with increasing nickel oxide concentration is observed. This systematic decrease is attributed to a change in the bonding characteristics between nickel(II) and the coordinating phosphate groups from mainly ionic to a small but significant contribution of covalent bonding. A similar effect is observed in the electronic absorption spectra of glasses showing a decrease of the Racah parameter B for the Ni^{2+} ions.

Key words: XANES; EXAFS; UV/VIS/NIR Spectroscopy; Sodium Metaphosphate Glasses; Metal-ligand Interaction.

1. Introduction

The color of phosphate glasses doped with transition metal oxides (“microcosmic salt beads”) is used as a tool in macro and semimicro qualitative inorganic analysis to detect transition metals [1–3]. Astonishingly, detailed studies on the origin of these colors are rarely found, and even fundamental information, like the oxidation state and coordination of the metal ions making up the chromophore, is frequently based on speculation [4]. Only recently we could show that the violet color of sodium metaphosphate glasses doped with manganese oxide is indeed caused by small amounts of Mn^{3+} ($\approx 3\%$ of the total manganese content) as assumed for a long time. However, the vast majority of manganese in such glasses adopts an oxidation state +II in agreement with the formula $(\text{NaPO}_3)_{1-x}(\text{MnO}_y)_x$ ($0.014 \leq x \leq 0.16$; $y \approx 1.03$) [5]. Even less information is available on structural and electronic aspects of the glass forming network. The

linkage of transition metal-oxygen coordination polyhedra $[\text{MO}_x]$ and phosphate groups, especially on a medium range scale, is experimentally not well investigated. Even the function of a transition metal oxide dopant as network builder or modifier according to Zachariassen’s concept is not always clear. For glasses $(\text{NaPO}_3)_{1-x}(\text{NiO})_x$ ($0.008 \leq x \leq 0.30$) a chemist might ask if these are sodium nickel phosphates or sodium phosphato-nickolates(II). This question is not only interesting in terms of IUPAC nomenclature rules, it pinpoints also the problem of variable covalency of the interaction between nickel(II) and the surrounding phosphate groups. The latter subject links our investigations to the physical meaning of empirically derived ligand-field parameters.

NiO-doped sodium metaphosphate glasses $(\text{NaPO}_3)_{1-x}(\text{NiO})_x$ ($0.008 \leq x \leq 0.30$) show a significant change in color from yellow to deep orange-brown with increasing concentration of the dopant. Similar variations in color are observed for crystalline

nickel(II) phosphates as a result of changes in the coordination number of Ni^{2+} and/or the connectivity of $[\text{NiO}_x]$ coordination polyhedra [6–9]. For nickel(II) oxide itself variation of color from green to yellowish-brown and even black is related to the presence of a small but significant amount of Ni^{3+} ions, giving rise to charge-transfer electronic transitions [10]. It is the aim of the present study to clarify the origin of the color of sodium metaphosphate glasses $(\text{NaPO}_3)_{1-x}(\text{NiO})_x$ and to get some insight into the structure of these glassy phosphates. For this purpose a combined investigation of the X-ray absorption fine structure (XAFS) and the electronic absorption spectra of several glassy phosphates $(\text{NaPO}_3)_{1-x}(\text{NiO})_x$ and some crystalline sodium-nickel(II) phosphates has been undertaken.

XANES spectra are widely used to determine the valency of transition metal ions in an unknown compound by comparison with crystalline reference samples [11–15]. Structural information, even of amorphous materials, can be obtained from EXAFS evaluations [5, 15–19]. Even hints on medium range order (MRO) might be taken from EXAFS, as has been shown for colloidal crystalline metal oxide clusters or even metal clusters within glasses [16, 17, 20–22]. For example, the evidence of ordered domains in NiO-containing low-alkali borate glasses has been shown by Cormier *et al.* [17]. This order is preserved in Ni-containing low-alkali borate glasses [17], whereas in the case of silicate glasses a reduced coordination is observed, revealing a mixing of four and five oxygen-coordinated sites [18].

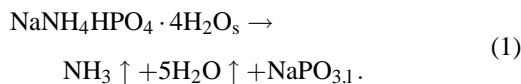
In this study, we present Ni K-edge XANES and EXAFS investigations, as well as electronic absorption spectra of a series of nine sodium metaphosphate glasses $(\text{NaPO}_3)_{1-x}(\text{NiO})_x$ ($0.008 \leq x \leq 0.30$) with varying amounts of NiO dopant. This is done in order to explain the origin of the changes of the color of the respective glassy samples, to get deeper insight into the ligand behavior of phosphate groups towards Ni^{2+} ions, and to get some information of the MRO in such glasses.

2. Experimental

2.1. Sample Preparation

For the present study, glasses $(\text{NaPO}_3)_{1-x}(\text{NiO})_x$ of nine different nickel oxide concentrations were prepared: $x = 0.008, 0.014, 0.033, 0.074, 0.10, 0.15, 0.20, 0.25,$ and 0.30 . Batches of about 30 g NaPO_3

melt were obtained by heating sodium ammonium hydrogenphosphate tetrahydrate (“microcosmic salt”, Merck, p.a.) in a gold crucible under occasional stirring at about 1073 K using a Bunsen burner. The decomposition was always accompanied by vigorous degassing of water and ammonia according to



After adding appropriate amounts of NiO (Aldrich, 99.9%) in small portions the melt was heated in air for 4 h at 1073 K in a chamber furnace and afterwards quenched between a metal plate and a metal block, both cooled with liquid nitrogen. Thus obtained glass plates (diameter: ~ 5 cm, thickness: ~ 3 mm) were annealed for another 4 h in a drying cabinet at 373 K to reduce thermal strain. Slow cooling of the melts $(\text{NaPO}_3)_{1-x}(\text{NiO})_x$ ($x \leq 0.30$) led to two-phase mixtures of crystalline sodium *catena*-metaphosphate [23] and “ $\text{Na}_2\text{NiP}_2\text{O}_7$ ” [24] in agreement with the phase equilibria in the quaternary system $\text{Na}_2\text{O}/\text{NiO}/\text{P}_4\text{O}_{10}$ [9]. The described quenching procedure did not allow synthesis of glasses $(\text{NaPO}_3)_{1-x}(\text{NiO})_x$ with $x > 0.30$. For such compositions, crystalline phases only were obtained.

With increasing content of nickel oxide, the glasses show a change in color from lemon-yellow to dark orange-brown. Above a dopant concentration of approximately 15%, no further change of color is visually recognized.

X-Ray powder diffraction using image plate-technique Guinier photographs [25–27] provided no hints for crystalline components present in the glasses.

For comparison, the crystalline sodium nickel(II) phosphates $\text{Na}_4\text{Ni}_3(\text{P}_2\text{O}_7)(\text{PO}_4)_2$ ($x = 0.429$) [28] and “ $\text{Na}_2\text{NiP}_2\text{O}_7$ ” ($x = 0.333$) [24], both belonging to the quasi-binary system $(\text{NaPO}_3)_{1-x}(\text{NiO})_x$, have been synthesized in a similar way. The crystalline phases, however, were obtained by slow cooling ($10^\circ/\text{h}$) to room temperature instead of rapid quenching [9].

Nickel monoxide, NiO (Sigma-Aldrich Chemie GmbH, black color), and nickel foil (Goodfellow) for reference XAFS measurements were purchased.

2.2. Optical Spectroscopy

Polarized single-crystal absorption spectra were measured using a modified CARY 17 spectrophotometer (Spectra Services, ANU Canberra). For a better signal to noise ratio the spectrophotometer is equipped

with a chopper (optical chopper, model SR540, Stanford Research Systems, Inc.) for modulation of the incident beam and a lock-in amplifier (model SR510, Stanford Research Systems, Inc.). For measurements in the near IR ($6,600 \text{ cm}^{-1}$ to $16,000 \text{ cm}^{-1}$) a liquid nitrogen-cooled Ge-photodiode detector (model 403, Applied Detector Corporation, Fresno, CA) was used. A photomultiplier (model PR-1400RF, Products for Research Inc.) was used as detector in the UV/VIS region ($12,000 \text{ cm}^{-1}$ to $32,000 \text{ cm}^{-1}$). The spectrophotometer is made for the measurement of polarized absorption spectra of rather small single-crystals having cross sections down to 0.1 mm. Further details about the spectrometer were published in [29, 30].

2.3. XAFS Measurements

XAFS measurements were performed at the beamline BN3 at the Electron Stretcher Accelerator (ELSA), Physikalisches Institut, University of Bonn [31]. The storage ring was operating at 2.3 GeV and currents ranged from 30 to 60 mA. A slightly modified Lemmonier-type double-crystal monochromator [32], equipped with a pair of Ge (220) crystals, was used. The Ni K-edge XANES spectra were measured in steps of 0.7 eV at the edge, EXAFS spectra in steps of approximately 1.5 eV. The samples were ground and fixed between two layers of self-adhesive Kapton tape. The sample thicknesses were optimized to result in an edge jump of approximately 1. The spectra were taken in transmission mode, incident and transmitted beam currents were recorded with ionization chambers under atmospheric air pressure and read out using Balzers QME311 electrometers. The linear absorption coefficient was calculated following the Lambert-Beer's law. For each data point, the integration time was set to 500 ms. Energy calibration was done by recording the spectrum of elemental nickel and setting the first inflection point of the main absorption edge to 8,333 eV, the bonding energy of the 1 s electron [33]. In case of the XANES spectra, a pre-edge background correction was done using a linear fit and the spectra were normalized to unity at 8,480 eV. EXAFS spectra were analyzed using the UWXAFS [34] and FEFF7 [35] suites of programs.

3. Results and Discussion

An arbitrary crystal face of $\text{Na}_4\text{Ni}_3(\text{P}_2\text{O}_7)(\text{PO}_4)_2$, showing dichroic behavior (yellow in “vpol” direction;

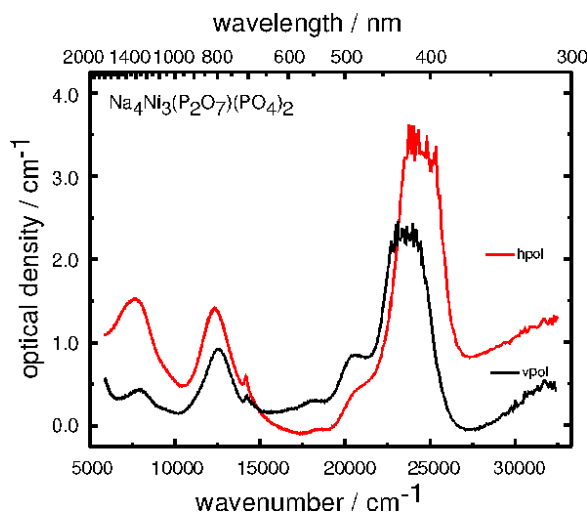


Fig. 1. $\text{Na}_4\text{Ni}_3(\text{P}_2\text{O}_7)(\text{PO}_4)_2$, polarized single-crystal electronic absorption spectra of an arbitrary crystal face. The “structure” in the maxima of the bands around $24,000 \text{ cm}^{-1}$ is due to high crystal thickness leading to high absorption and low signal intensity in this wavenumber range.

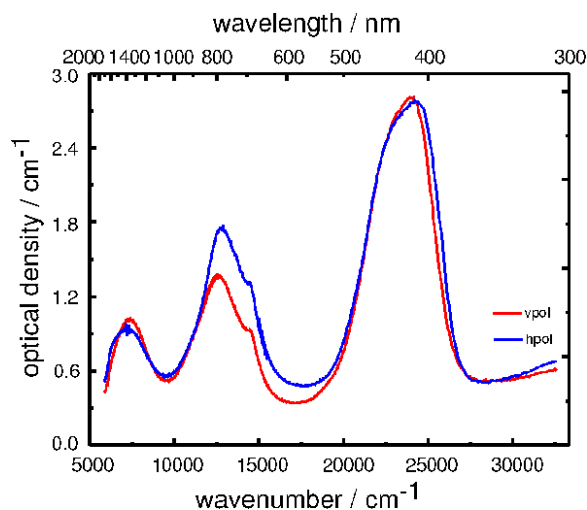


Fig. 2. “ $\text{Na}_2\text{NiP}_2\text{O}_7$ ”, polarized single-crystal electronic absorption spectra of an arbitrary crystal face.

dark yellow in “hpol” direction) under a polarizing microscope, has been used for the measurement of polarized single-crystal absorption spectra (Fig. 1). Due to the presence of chromophores $[\text{Ni}^{\text{II}}\text{O}_6]$ with high radial and angular distortion [28], significant band splittings are observed as a consequence of low-symmetry ligand field components. As a further effect of the low-symmetry ligand field experienced by the Ni^{2+} ions, the spin-forbidden transitions ${}^3\text{A}_{2g} \rightarrow {}^1\text{E}_g(\text{D})$ ($\nu \approx$

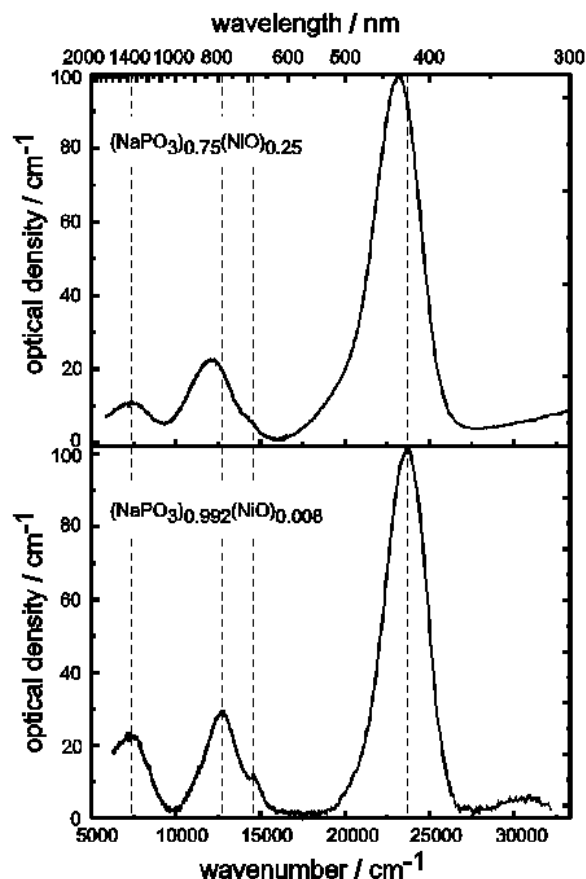


Fig. 3. Electronic absorption spectra of glasses $(\text{NaPO}_3)_{1-x}(\text{NiO})_x$ ($x = 0.008$, bottom, and 0.25 , top) in the UV/VIS/NIR region.

$14,500 \text{ cm}^{-1}$) and ${}^3\text{A}_{2g} \rightarrow {}^1\text{T}_{2g}(\text{D})$ ($\nu \approx 18,000 \text{ cm}^{-1}$ and $\nu \approx 20,500 \text{ cm}^{-1}$) are well resolved with rather high intensity due to intensity-stealing enforced by spin-orbit coupling.

Crystals of “ $\text{Na}_2\text{NiP}_2\text{O}_7$ ” show no polychroic behavior, as is reflected by the absorption spectra taken from an arbitrary crystal face (Fig. 2). Apart from a rather broad band observed for the transition ${}^3\text{A}_{2g} \rightarrow {}^3\text{T}_{1g}(\text{P})$, no more evidence for low-symmetry ligand field components is found. The absorption assigned to the spin-forbidden transition ${}^3\text{A}_{2g} \rightarrow {}^1\text{E}_g(\text{D})$ is far less pronounced than in $\text{Na}_4\text{Ni}_3(\text{P}_2\text{O}_7)(\text{PO}_4)_2$.

Polished slices that were cut from the glass plates $(\text{NaPO}_3)_{1-x}(\text{NiO})_x$ have been measured at room temperature. Representative spectra for glasses with low ($x = 0.008$) and high ($x = 0.25$) dopant concentration are contained in Figure 3. The spectra show the electronic transitions ${}^3\text{A}_{2g} \rightarrow {}^3\text{T}_{2g}(\text{F})$ ($\nu_1 \approx 7,400 \text{ cm}^{-1}$),

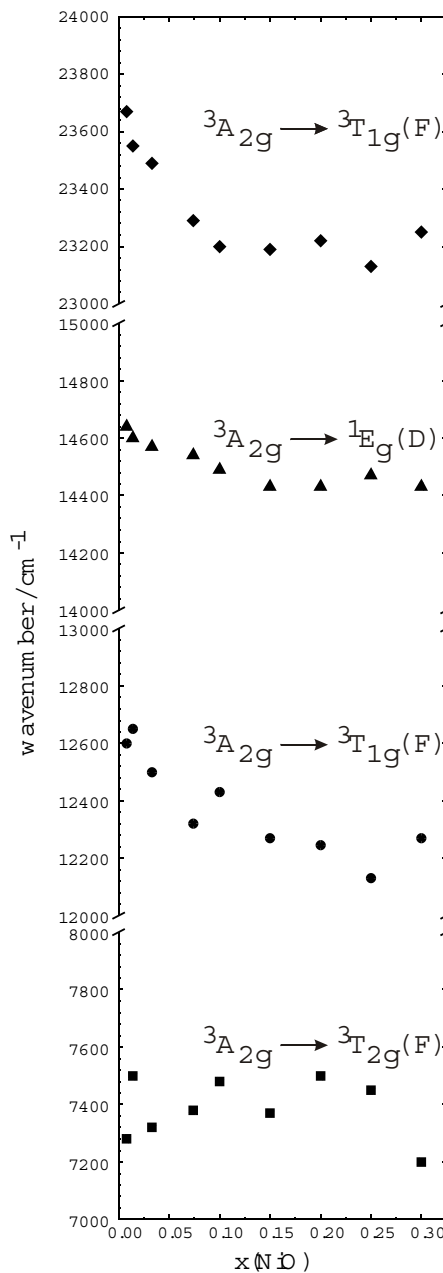


Fig. 4. Summary of electronic transition energies observed for glasses $(\text{NaPO}_3)_{1-x}(\text{NiO})_x$ ($0.008 \leq x \leq 0.30$).

${}^3\text{A}_{2g} \rightarrow {}^3\text{T}_{1g}(\text{F})$ ($\nu_2 \approx 12,400 \text{ cm}^{-1}$), ${}^3\text{A}_{2g} \rightarrow {}^1\text{E}_g(\text{D})$ ($\nu_3 \approx 14,500 \text{ cm}^{-1}$), and ${}^3\text{A}_{2g} \rightarrow {}^3\text{T}_{1g}(\text{P})$ ($\nu_4 \approx 23,300 \text{ cm}^{-1}$) typically observed for an octahedral $[\text{Ni}^{\text{II}}\text{O}_6]$ chromophore [8, 36]. The energies of the electronic transitions have been visually estimated for all glasses. Figure 4 gives a summary of the observed

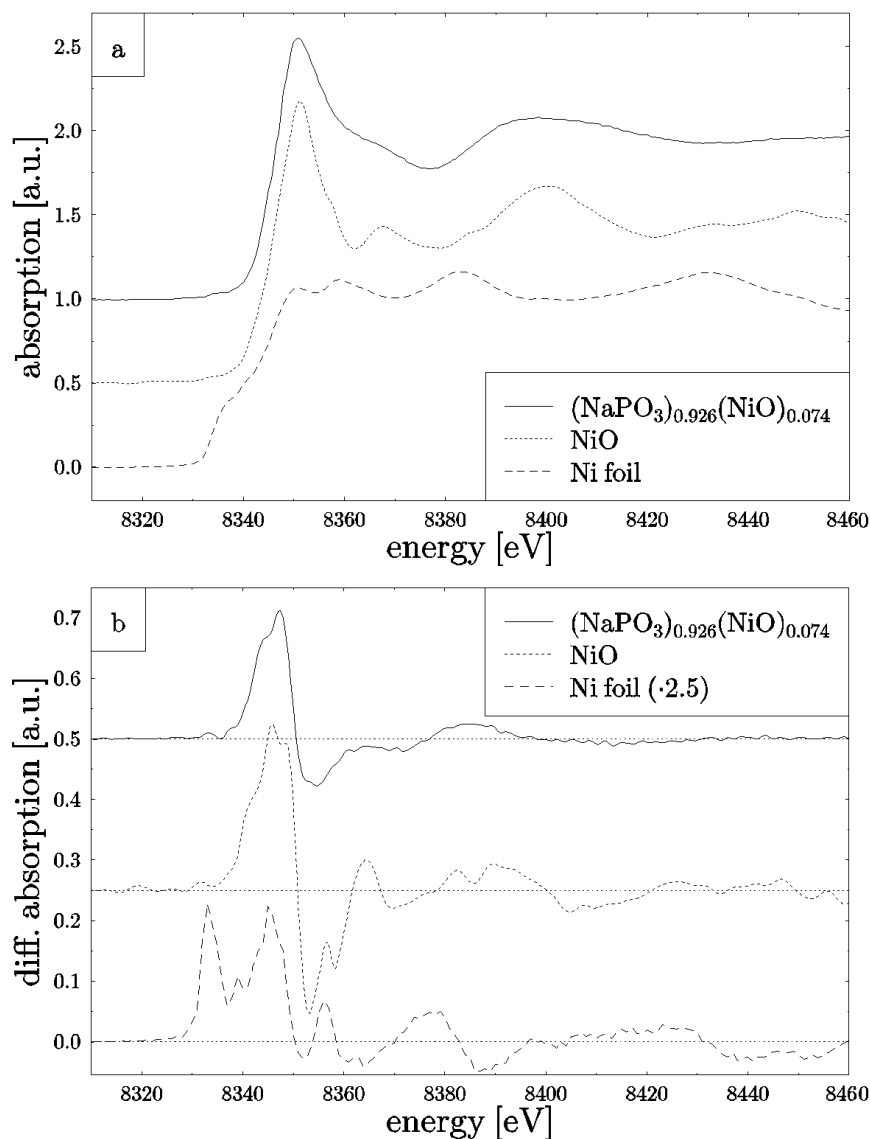


Fig. 5. XANES measurements (a) and derivatives (b) of Ni foil, NiO, and $(\text{NaPO}_3)_{0.926}(\text{NiO})_{0.074}$ glass. The spectra are shifted along the y axis for clarity.

transition energies for all glasses. A red shift of transitions ν_2 , ν_3 , and ν_4 with the NiO concentration increasing from $x = 0.008$ to $x = 0.15$ is clearly visible. At higher dopant concentration no further shift is observed for these transitions. In addition to the band shifts, an increasing asymmetry and broadening is observed at higher NiO concentrations for the absorption band ν_4 and to a much lesser extend for band ν_2 . It is quite remarkable that the absorption band ν_4 in glasses of low dopant concentration is even sharper than the corresponding band in the crystalline phosphates “ $\text{Na}_2\text{NiP}_2\text{O}_7$ ” and $\text{Na}_4\text{Ni}_3(\text{P}_2\text{O}_7)(\text{PO}_4)_2$. This might

be taken as an indication for the presence of rather high-symmetric octahedral chromophores $[\text{Ni}^{\text{II}}\text{O}_6]$ in these glasses. Within the accuracy of determination, the energy of transition ν_1 , which is equal to the ligand-field splitting Δ_o for Ni^{2+} ions in octahedral coordination, shows no dependence on the NiO concentration.

As a next step to analyze the electronic structure of a transition metal-containing glass, it is useful to determine the valency of the respective metal ions, because the investigation of sodium metaphosphate glasses doped with manganese oxides impressively demonstrated that assumptions derived only from the

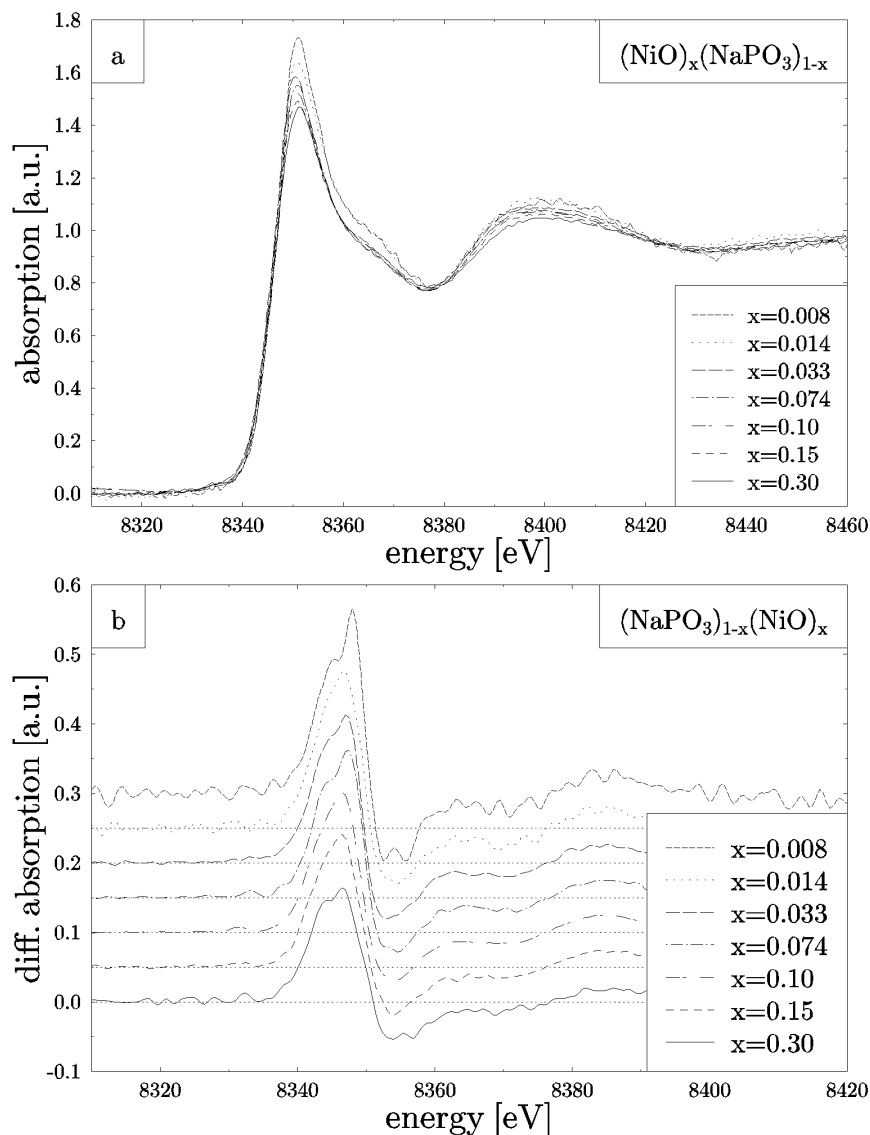


Fig. 6. XANES measurements (a) and derivatives (b) of seven NiO-doped glasses.

color of the glass might be misleading [5]. Within the mentioned investigation, the valency of the manganese ions was determined to be in the majority +II, in contrast to the violet color of the glasses which arises from approximately 3% Mn^{3+} ions.

A well established method to gain information about the oxidation state of transition metal ions in unknown compounds is to compare the shift of the main absorption edge of the respective XANES spectra with crystalline reference samples, as the absorption edges shift to higher energies with increasing valency of the ions [5, 12–15]. Figure 5a shows the Ni K-edge

XANES spectra of the elemental nickel foil, nickel oxide and the spectrum of the $(\text{NaPO}_3)_{0.926}(\text{NiO})_{0.074}$ glass, the first derivatives of the respective spectra are presented in Figure 5b. The shift in the position of the first inflection point of the glass spectrum with respect to the nickel foil measurement is 15.0(7) eV and therefore very close to the shift of the nickel monoxide spectrum, which is 13.0(7) eV. The errors given are estimated to be in the order of magnitude of one monochromator step in the measuring routine. Figure 6a shows the XANES spectra of all seven examined NiO-doped sodium metaphosphate glasses. The

Table 1. XANES spectra of NiO and glasses $(\text{NaPO}_3)_{1-x}(\text{NiO})_x$. Energy shifts and observed areas. Error margins are ± 0.7 eV for energy shifts and ± 0.5 a. u. for observed areas, respectively.

Sample	NiO	x						
		0.008	0.014	0.033	0.074	0.10	0.15	0.30
Shift (eV)	13.0	15.0	14.0	14.0	14.5	13.5	13.5	13.5
Area (a.u.)	–	37.6	37.5	36.3	35.4	34.9	34.5	34.4

first derivatives are presented in Figure 6b. The shifts in the position of the absorption edges are close the error margins, clearly indicating that the Ni ions are Ni^{2+} throughout all seven examined glasses. The values of the respective energy shifts are listed in Table 1. Therefore, we conclude that the changes in the color are not due to the presence of Ni ions of higher valency than +II within the glasses. This conclusion is supported by the optical transparency of the glasses in the near UV at wavenumbers above ca. $26,000 \text{ cm}^{-1}$ (Fig. 3). As has been shown [10], the presence of even traces of nickel in higher oxidation states than +II would give rise to strong absorption bands in this spectral region due to oxygen-nickel charge-transfer transitions.

However, concentration dependent changes are clearly visible within the XANES spectra as well as in the optical spectra. A decrease in intensity of the white line with increasing nickel content is observed. When calculating the area underneath the recorded spectra in an energy range from 8,320 eV, shortly before the edge, to 8,375.5 eV, the first pronounced minimum after the main absorption edge, a decrease of approximately 10% from the lowest to the highest NiO-doped glass arises. The absolute values calculated are also listed in Table 1.

To evaluate whether changes in the geometrical bonding of the nickel ions might be responsible for this systematic decrease, EXAFS spectra have been recorded for seven NiO-doped sodium metaphosphate glasses. The k^3 -weighted $\chi(k)$ -functions of the seven glasses are shown in Fig. 7a and the FTs are presented in Figure 7b. Already at this stage of analysis, it can be stated qualitatively that there are no significant changes in the bonding geometry of the nickel sites because of the similarity of the presented data.

As a reference study to the analysis of the glasses, the EXAFS spectrum of nickel monoxide, also presented in Fig. 7, was evaluated using the UWXAFS package [34]. Therefore, the k^3 -weighted $\chi(k)$ -function was Fourier transformed in the wave-vector range $2.7 \leq k \leq 8.7 \text{ \AA}^{-1}$. For the NiO reference system, the modulus of the FT is dominated by scatter-

Table 2. Structural parameters of glasses $(\text{NaPO}_3)_{1-x}(\text{NiO})_x$ obtained by EXAFS measurements.

x	C.N. _{Ni-O}	$R_{\text{Ni-O}}$ [Å]	$\sigma_{\text{Ni-O}}^2$ [Å ²]	C.N. _{Ni-P}	$R_{\text{Ni-P}}$ [Å]	$\sigma_{\text{Ni-P}}^2$ [Å ²]
0.008	5.9(1.0)	2.08(2)	0.006(4)	6.0(1.0)	3.23(2)	0.011(3)
0.014	5.8(1.0)	2.06(2)	0.005(2)	6.0(1.0)	3.27(2)	0.010(1)
0.033	6.1(1.0)	2.05(2)	0.007(1)	6.0(1.0)	3.24(2)	0.012(3)
0.074	6.0(1.0)	2.07(2)	0.008(1)	6.0(1.0)	3.26(2)	0.013(1)
0.10	6.0(1.0)	2.05(2)	0.008(1)	6.0(1.0)	3.21(2)	0.014(2)
0.15	6.0(1.0)	2.04(2)	0.006(1)	6.0(1.0)	3.17(2)	0.013(2)
0.30	6.0(1.0)	2.05(2)	0.009(1)	6.0(1.0)	3.17(2)	0.018(2)

ing at the six first-shell Ni-O and twelve second-shell Ni-Ni neighbors. The FT was fitted in the range 1.1 – 3.3 Å, using amplitude factors, phase shifts and electron mean-free paths determined by the FEFF7 program [35], and the structural information of NiO reported by Schmahl and Eikerling [37]. Coordination numbers and the distances $d(\text{Ni-O}) = 2.089 \text{ \AA}$ and $d(\text{Ni-Ni}) = 2.954 \text{ \AA}$ were kept fixed. The fitting result is shown in Figure 7b. It revealed an amplitude reduction factor, S_0^2 , of 0.85 which was used without adjustment in the analysis of the glass data. The first-shell Ni-O contributions of the glasses were fitted in the range 1.2 – 2.0 Å after Fourier transformation in the range $3.2 \leq k \leq 11 \text{ \AA}^{-1}$ using the Ni-O path parameters mentioned above. The results are summarized in Table 2. The fits are also shown in Figure 7b.

Within the error margins, the structural parameters of all seven investigated glasses are almost equal, showing a mean Ni-O coordination of approximately 6.0(1.0) at a distance of 2.06(2) Å and a Debye-Waller factor of 0.007(1) Å², which leads to the conclusion that the Ni^{2+} ions are octahedrally surrounded by six oxygen atoms. These results exclude changes in the coordination number of Ni^{2+} ions from C.N.(Ni^{2+}) = 6 at lower NiO concentrations to C.N.(Ni^{2+}) = 5 at higher NiO concentrations. The observed average distance $d(\text{Ni-O}) = 2.06(2) \text{ \AA}$ agrees well with values observed by X-ray single crystal studies of many nickel(II) phosphates [8]. A simple geometrical explanation for the changes in the color and differences stated for the XANES spectra of glasses $(\text{NaPO}_3)_{1-x}(\text{NiO})_x$ can not be given, in contrast to the case of MnO_y -doped sodium metaphosphate glasses, where a similar change was attributed to a mixing of 6-fold and 4-fold oxygen coordination [5]. In addition, it is worth mentioning that the distances of the first-shell oxygen coordination do not decrease systematically with increasing Ni concentration as reported for $\text{Ni}_c\text{Mg}_{1-c}\text{O}$ solid solutions [19] and the Debye-Waller factors are comparable over the whole series of glasses, which leads to the assumption that the geometrical structure of the nickel

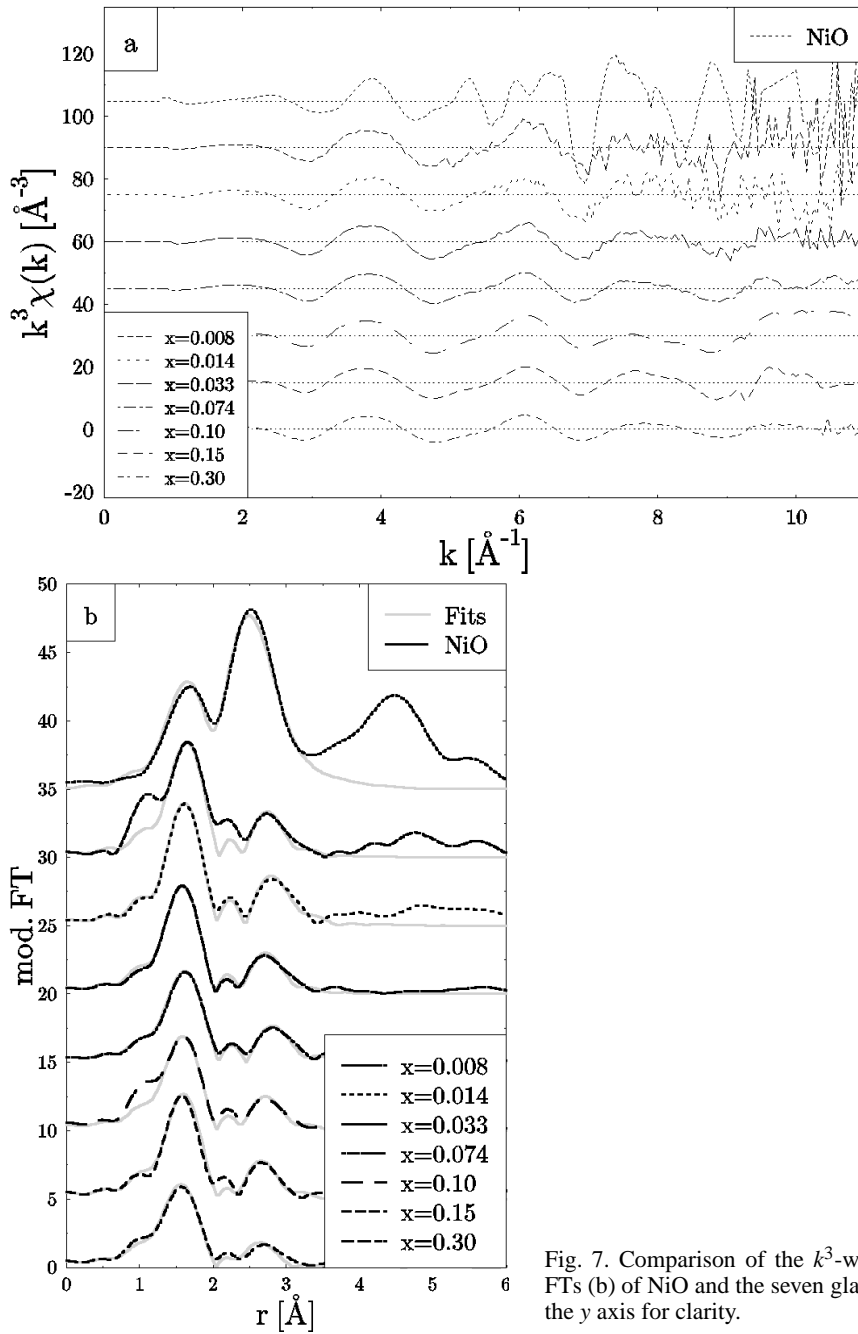


Fig. 7. Comparison of the k^3 -weighted $\chi(k)$ -functions (a) and the FTs (b) of NiO and the seven glasses. The data sets are shifted along the y axis for clarity.

sites does not depend significantly on the Ni concentration.

An evaluation of the second-shell scattering contributions was performed in the range 2.0–3.2 Å. Stable results were gained for fitting with phosphorus atoms only. Assuming an average of 6.0(1.0) phospho-

rus neighbors, an approximate distance of 3.22(2) Å and an average Debye-Waller factor of 0.013(2) Å² is found. Path parameters for the phosphorus backscatterers were derived from FEFF7-calculations of α -Ni₂P₂O₇ [38]. The addition of oxygen and/or nickel backscatterers or replacing phosphorus with either one

or both of these types of atoms does not provide physically meaningful results. At this point, one should emphasize that this implies that there is no evidence of NiO-containing ordered domains in the investigated phosphate glasses, in contrast to the observation reported by Cormier *et al.* for NiO-containing low-alkali borate glasses [17]. This result prohibits the explanation of the color of the samples as to result from scattering of light at colloidal crystalline nickel centers within the investigated glasses. Instead, we explain the decrease in white line intensity with a modification of the bonding characteristics of the nickel atoms from mainly ionic to more pronounced covalent. It is a well known characteristic of 3d-metal compounds that the formation of a covalent bond not only causes a reduced electron density of states of the 3d-orbitals but is accompanied by a filling of the metals anti-bonding p-type orbitals [39, 40]. As the white line intensity of K-edge XANES spectra is related to the unoccupied p-type electron density of states, the decrease in white line intensity is traced back to a more pronounced covalent bonding between Ni^{2+} ions and the surrounding phosphate groups. Nevertheless, this effect is not strong enough to lead to a shift of the position of the main absorption edge as reported in the comparison of the ionic NaCl with respect to partly covalent PdCl_2 [41]. On the other hand, the electronic spectra of glasses $(\text{NaPO}_3)_{1-x}(\text{NiO})_x$ (Figs. 3 and 4) indicate also increasing covalency for the interaction between the 3d-orbitals of nickel and the phosphate groups with increasing NiO concentration. The variation of the bonding situation for nickel(II) finds also its counterpart in the chemical behaviour, namely the solubility of such glasses. Sodium metaphosphate glasses doped with low NiO concentrations can easily be dissolved in water, while higher dopant concentration leads to slower dissolution rates.

4. Conclusions

The XANES investigation of a series of sodium metaphosphate glasses, doped with different amounts of NiO, and reference compounds show that nickel ions within the glasses are Ni^{2+} , independent of the NiO concentration. The XANES spectra show a decrease of white line intensity with increasing NiO concentration. This effect can not be traced back to

changes in the geometrical bonding situation of the nickel ions, evaluated by EXAFS analysis of the first and second coordination shell. Instead, the observed decrease of white line intensity is explained by a change in the electronic bonding situation of the nickel ions. With increasing NiO concentration bonding between Ni^{2+} and the surrounding six phosphate groups changes from mainly ionic to a significantly covalent interaction. These results of the XANES and EXAFS investigations are nicely matched by the evaluation of the electronic spectra measured for glasses $(\text{NaPO}_3)_{1-x}(\text{NiO})_x$ and the crystalline reference compounds “ $\text{Na}_2\text{NiP}_2\text{O}_7$ ” and $\text{Na}_4\text{Ni}_3(\text{P}_2\text{O}_7)(\text{PO}_4)_2$ in the UV/VIS/NIR region. The electronic spectra show clearly that the ligand-field splitting Δ_o observed for the $[\text{Ni}^{\text{II}}\text{O}_6]$ chromophore is not significantly depending on the NiO concentration in the glasses. The red shift (Figs. 3 and 4) observed for bands ν_2 , ν_3 , and ν_4 , giving rise to the change of the color from yellow to dark-orange, can be correlated to a change of the Racah Parameter B [36]. To our knowledge it is the first time that experimental evidence for increasing covalency of metal-ligand interaction has been observed for the same compounds in XANES and in electronic absorption spectra. Though due to interaction between ligand orbitals and different metal orbitals (4p-orbitals for XANES; 3d-orbitals for electronic spectra), it appears quite reasonable that this effect is observed by both methods. Clearly these results indicate a change in the metal ligand interaction from basically ionic to increasingly covalent with increasing NiO concentration in the glasses. In addition, the color change is caused by the broadening of the absorption band ν_4 assigned to the transition ${}^3A_{2g} \rightarrow {}^3T_{1g}(\text{P})$. It has already been noted that absorption band ν_4 for the glass with composition $(\text{NaPO}_3)_{0.992}(\text{NiO})_{0.008}$ (Fig. 3) is even smaller than ν_4 for the crystalline nickel phosphates (Figs. 1 and 2). This implies radial and angular distortions for the $[\text{Ni}^{\text{II}}\text{O}_6]$ chromophore in $(\text{NaPO}_3)_{0.992}(\text{NiO})_{0.008}$ to be significantly less than in the crystalline reference compounds, where one finds $1.99 \text{ \AA} \leq d(\text{Ni-O}) \leq 2.23 \text{ \AA}$ and $68.3^\circ \leq \angle(\text{O,Ni,O}) \leq 103.2^\circ$ [24, 28].

Acknowledgement

The authors appreciate the financial support by the Deutsche Forschungsgemeinschaft (DFG) within the Sonderforschungsbereich (SFB) 408.

- [1] G. Ackermann and D. Hesse, *Z. Anorg. Allg. Chem.* **323**, 149 (1963).
- [2] G. Svehla, *Vogel's Textbook of Macro and Semimicro Qualitative Inorganic Analysis*, Longman Group, London 1979.
- [3] W. A. Weyl, *Coloured Glasses*, Soc. Glass Techn., Sheffield 1999.
- [4] U. Kohlberg, in: *The Properties of Optical Glasses* (Eds. H. Bach and N. Neuroth), Schott Series on Glass and Glass Ceramics, Springer Verlag, Heidelberg 1998.
- [5] N. Zotov, H. Schlenz, B. Brendebach, H. Modrow, J. Hormes, F. Reinauer, R. Glaum, A. Kirfel, and C. Paulmann, *Z. Naturforsch.* **58a**, 419 (2003).
- [6] K. Maaß, Ph. D. thesis, University of Gießen 2002.
- [7] B. El-Bali, A. Boukhari, J. Aride, K. Maaß, D. Wald, R. Glaum, and F. Abraham, *Solid State Sciences* **3**, 669 (2001).
- [8] M. Funke, M. Blum, R. Glaum, and B. El-Bali, *Z. Anorg. Allg. Chem.* **630**, 1040 (2004).
- [9] M. Funke, part of planned Ph. D. thesis, University of Bonn.
- [10] V. Propach, D. Reinen, H. Drenkhahn, and H. Müller-Buschbaum, *Z. Naturforsch.* **33b**, 619 (1978).
- [11] B. Brendebach, F. Reinauer, N. Zotov, M. Funke, R. Glaum, J. Hormes, and H. Modrow, *J. Non-Cryst. Solids* **351**, 1072 (2005).
- [12] B. K. Agarwal and L. P. Verma, *J. Phys. C: Solid State Phys.* **3**, 535 (1970).
- [13] A. K. Nigam and M. K. Gupta, *J. Phys. F: Metal Phys.* **3**, 1251 (1973).
- [14] S. I. Salem, C. N. Chang, P. L. Lee, and V. Severson, *J. Phys. C: Solid State Phys.* **11**, 4085 (1978).
- [15] A. N. Mansour and C. A. Melendres, *J. Phys. Chem. A* **102**, 65 (1998).
- [16] F. d'Acapito, S. Mobilio, G. Battaglin, E. Cattaruzza, F. Gonella, F. Caccavale, P. Mazzoldi, and J. R. Regnard, *J. Appl. Phys.* **87**, 1819 (2000).
- [17] L. Cormier, L. Galois, and G. Calas, *Europhys. Lett.* **45**, 572 (1999).
- [18] L. Galois and G. Calas, *Geochim. Cosmochim. Acta* **57**, 3613 (1993).
- [19] A. Kuzmin, N. Mironov, J. Purans, and A. Rodionov, *J. Phys.: Condens. Matter* **48**, 9357 (1995).
- [20] F. Garridot, F. Caccavale, F. Gonella, and A. Quaranta, *Pure Appl. Opt.* **4**, 771 (1995).
- [21] F. Gonella, F. Caccavale, L. D. Bogomolova, F. d'Acapito, and A. Quaranta, *J. Appl. Phys.* **83**, 1200 (1998).
- [22] S. Padovani, C. Sada, P. Mazzoldi, B. Brunetti, I. Borgia, A. Sgamellotti, A. Giulivi, F. d'Acapito, and G. Battaglin, *J. Appl. Phys.* **93**, 10058 (2003).
- [23] A. McAdam, K. H. Jost, and B. Beagley, *Acta Crystallogr. B* **24**, 1621 (1968).
- [24] F. Erragh, A. Boukhari, F. Abraham, and B. Elouadi, *J. Solid State Chem.* **152**, 323 (2000).
- [25] Y. Amemiya and J. Miyahara, *Nature* **336**, 89 (1988).
- [26] J. Miyahara, *Chem. Today* **223**, 29 (1989).
- [27] K. Maaß, R. Glaum, and R. Gruehn, *Z. Anorg. Allg. Chem.* **628**, 1663 (2002).
- [28] F. Sanz, C. Prada, J. M. Rojo, and C. Ruíz-Valero, *Chem. Mater.* **13**, 1334 (2001).
- [29] E. Krausz, *AOS News* **12**, 21 (1998).
- [30] E. Krausz, *Aust. J. Chem.* **46**, 1041 (1993).
- [31] K. H. Althoff, W. v. Drachenfels, A. Dreist, D. Husmann, M. Neckenig, H.-D. Nuhn, W. Schauerer, M. Schillo, F. J. Schittko, and C. Wermelskirchen, *Part. Accel.* **27**, 101 (1990).
- [32] M. Lemmonier, O. Collet, C. Depautex, J.-M. Esteva, and D. Raoux, *Nucl. Instr. Meth. A* **152**, 109 (1978).
- [33] G. P. Williams, in: *X-Ray Data Booklet* (Eds. A. C. Thompson and D. Vaughan), Lawrence Berkeley Laboratory, Berkeley 2001.
- [34] E. A. Stern, M. Newville, B. Ravel, D. Haskel, and Y. Yakobi, *Physica B* **208–209**, 117 (1995).
- [35] S. I. Zabinsky, J. J. Rehr, A. Ankudinov, R. C. Albers, and M. J. Eller, *Phys. Rev. B* **52**, 2995 (1995).
- [36] A. B. P. Lever, *Inorganic Electronic Spectroscopy*, Elsevier Publ., Amsterdam 1986.
- [37] N. G. Schmahl and G. F. Eikerling, *Z. Phys. Chem.* **62**, 268 (1964).
- [38] K. Lukaszewicz, *Bull. Acad. Pol. Sci., Sci. Chim.* **15**, 47 (1967).
- [39] T. Hatsui, Y. Takata, and N. Kosugi, *Chem. Phys. Lett.* **284**, 320 (1998).
- [40] T. Hatsui, Y. Takata, and N. Kosugi, *J. Elec. Spec. Rel. Phen.* **103**, 827 (1999).
- [41] S. Bucher, Ph. D. thesis, University of Bonn, 2002.